

# Improved Electrochemical Preparation of Nano Porous-Graphene Oxide Edge Like Electrode for Cerium/Vanadium Redox Flow Batteries

Muthuraman Govindan and Il-Shik Moon\*

Department of Chemical Engineering, Sunchon National University, 315 Maegok Dong, Suncheon 540-742, Chonnam, Republic of Korea

\*E-mail: [ismoon@suncon.ac.kr](mailto:ismoon@suncon.ac.kr)

Received: 5 August 2013 / Accepted: 29 August 2013 / Published: 25 September 2013

---

A nano porous-graphene oxide edge like (NP-GO<sub>el</sub>) electrode is presented as an electrochemical active material for Ce(IV)/Ce(III) redox couples for Ce-V redox flow batteries. The medium used to prepare NP-GO<sub>el</sub> electrode was 2 M NH<sub>3</sub> + 2% 2 M H<sub>2</sub>SO<sub>4</sub> + 1% triton-100. The morphology and electrochemical properties of NP-GO<sub>el</sub> electrode were investigated by atomic force microscopy analysis, X-ray photoelectron spectroscopy, and cyclic voltammetry. Surface characterization results showed that that NP-GO<sub>el</sub> electrode possesses nanopores containing hydroxyl (R-OH) and epoxy (C-O-C) groups. This increase of nano pores containing oxygen functional groups provided excellent electrocatalytic activity towards Ce(IV)/Ce(III) redox couples, whereas normally activated and prepared in 2 M NH<sub>3</sub> medium graphite showed sluggish quasi-reversible electron transfer activity towards Ce(IV)/Ce(III), suggesting that the Ce(IV)/Ce(III) redox reaction depends strongly on oxygen-containing groups generated on the surface of graphite and nano pores. When NP-GO<sub>el</sub> electrodes were modified with Nafion, electrode stability markedly increased with no change in electrode morphology. The electrochemically prepared NP-GO<sub>el</sub> shows promise for Cerium redox properties in Ce-V redox flow battery applications.

---

**Keywords:** Redox flow battery, in-situ preparation of GO, NP-GP<sub>el</sub>, galvanostatic method.

## 1. INTRODUCTION

Charge/discharge reactions in the redox flow batteries (RFB) are based entirely on redox reactions between soluble ionic species, in contrast to those of common secondary batteries, which utilize solid active materials. Accordingly, a long cycle life can be expected for rechargeable cells [1,2]. In particular, vanadium redox flow batteries (VRB) have received considerable attention during the past few years as promising candidates for applications in remote area power systems, wind turbine

generators, load leveling at electric power stations, and for emergency back-up applications [3]. VRBs use  $\text{VO}_2^+/\text{VO}^{2+}$  and  $\text{V}^{2+}/\text{V}^{3+}$  redox couples in acid medium as the positive and negative half-cell electrolytes, respectively, which is most their most important advantage [2]. These batteries have an open circuit voltage of approximately 1.26 V in the 100% charge state [4]. In order to increase the open circuit voltage or energy efficiency, combinations of metal ions have been used, such as, iron–chromium [5], all vanadium [6], zinc–ferricyanide [7], vanadium–cerium [8], and zinc–cerium [9]. Both vanadium [10] and cerium [11] are advantageous for energy storage due to their relatively large (1.56 V vs SHE) standard electrode potentials in aqueous media [12–14].

Many carbon based materials have been used as the VRB electrode materials, such as, carbon felts [15], carbon cloth [16], graphite powder [17], and carbon black [18]. However, these materials show poor reversibility towards redox couples. In cerium–vanadium RFBs, cerium oxidation has been reported for carbon electrodes [19], but stability over long periods of usage is questionable due to the high oxidation potential of Ce(III). Because of this high oxidation potential, carbon particles dissolution started from carbon anodes into acid electrolytes and become not usable anode [20]. However, conducting polymer coated electrode materials have minimized the carbon particle dissolution [21] as composite electrodes [22], but reversibility of mediator ion still lacking. In related with catalytic activity, in electrochemistry redox kinetics, oxygen functional groups are considered as more eminent catalyst on carbon electrodes [23]. Few publications using grapheme [24], graphite oxide [25], and graphene oxide [26, 27] pre-modified like ‘multilayer graphene nanoplatelet [28]’ on carbon electrodes where graphene oxides are synthesized by chemical way, in the RFB field were used to increase redox kinetics of metal ions. In-situ generation of oxygen groups on carbon surface can be an alternative and Hu et al., have adopted with the aim to use the electrochemical preparation of graphite oxide [29] but their focus mainly on graphene oxide that were dispersed in solution. To have properties similar to those of graphene oxide in solution, the surfaces of electrochemically prepared graphite electrode should be graphene oxide like nature such as nano porous with oxides on edge planes of each graphite particle. Only one report has focused on in-situ formation of graphene oxide nanosheet [30] and its application to sensor. Still more rooms are there to continue for detailed and different experimental way to prepare nano porous graphene oxide electrode using simple experimental techniques especially to prepare industrial type of electrode. Here in, we demonstrates an improved galvanostatic method, for preparation of graphene oxide edge like electrode with nano porous nature and their performances were investigated as active anode materials towards cerium redox couples in Ce–V RFBs.

## 2. EXPERIMENTAL

### 2.1. Preparation of nano porous graphite oxide edge like electrode

Nano-porous graphite oxide electrodes were prepared using a modification of an existing procedure [29], that is, a different electrolyte medium and applied potential. The experimental setup is shown in Fig.1. Two identical graphite electrodes (5 mm diameter) (purchased from Sigma-Aldrich),

as anode and cathode, were inserted in electrolyte medium containing 2 M  $\text{NH}_3$  + 2M 2%  $\text{H}_2\text{SO}_4$  + 1% TritonX-100. A constant potential (CP) (DC 7.5 V) was applied to the electrodes using a DC power source (Korea Switching Instruments). The anodic graphite rod was gradually oxidized and exfoliated into solution. The colorless electrolyte solution became brown within 5 hrs of operation. In addition, some coarse particles exfoliated from the graphite matrix and precipitated on the bottom of the container. After 5 hrs, the electrolysis process was terminated and the resultant electrode and dispersion were used for further investigations.

Modification of the NP-GO<sub>el</sub> electrodes was done using 5% Nafion solution by spread coating. Nafion (5  $\mu\text{l}$  of a 5% solution) was spread slowly to cover the electrode surface completely and then air dried for electrochemical analysis.

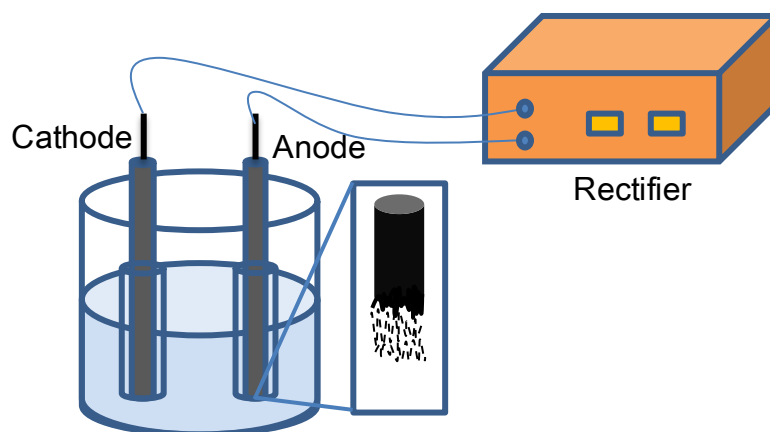


**Figure 1.** Schematic representation of the electrochemical preparation of nano pores-graphene oxide edge like (NP-GO<sub>el</sub>) electrode.

## 2.2. Characterization of dispersed solution and electrode

A UV-vis spectrophotometer (UV1600) was used to monitor the exfoliated carbon particles in the solution. Also, High-resolution transmission electron microscopy (HRTEM) images were obtained for carbon particle dispersed solution using a JEOL JEM-2000EX2 microscope operated at 200 kV. Solutions for HRTEM analysis were sonicated for 2 min and deposited on a copper grid. The surface morphologies and compositions of the prepared electrode materials were studied using a Hitachi S-4800 field-emission high-resolution scanning electron microscope (HRFESEM, accelerating voltage (5.0 kV) equipped with an energy-dispersive x-ray spectroscopy (EDS) setup. Atomic force microscope (AFM) experiments were performed using a nanoscope IVA multimode AFM equipped with a J-scanner and current-sensitive attachment (Digital Instruments, Santa Barbara, CA). Contact mode etched silicon probes with a cobalt-chrome coating were used for AFM measurements. X-ray photoelectron spectroscopy (XPS) data was obtained using an ESCALab220i-XL electron spectrometer from VG Scientific using 300W Al K  $\alpha$  radiation. The base pressure was  $\sim 3 \times 10^{-9}$  mbar. After subtracting the base line (Shirley-type), curve fitting was performed by using a mixed Gaussian/Lorentzian peak shape of variable proportion.

### 2.3. Electrochemical measurements

Cyclic voltammograms were obtained using a three-electrode electrochemical cell and a PAR 265 Electrochemical Workstation, USA. Prepared NP-GO<sub>el</sub> electrodes (5mm diameter) served as working electrodes. All potentials were measured using a platinum counter electrode and an Ag/AgCl reference electrode. The electrolyte used was a 1 M Ce(III) solution containing 2 M CH<sub>3</sub>SO<sub>3</sub>H (MSA) (as supporting electrolyte). All tests were performed in presence of dissolved oxygen to mimic real applications.

## 3. RESULTS AND DISCUSSION

### 3.1 Solution characterization

Fig. 2A shows the UV–vis absorption of exfoliated solution from graphite electrode. Two peaks were observed at 219 and 260 nm. The first peak at 219 nm provided an indication of nano-meter scale ( $10^{-9}$ ) of carbon particles [31] and the other at 260 nm indicates the formation of oxide on nano-particles [32]. Fig.2B shows the TEM image of exfoliated graphite particles in solution; particle sizes were  $\sim 70$  nm. These two studies indicated that the electrochemically prepared graphite particles in solution were nano-sized. Additionally, as mentioned previously [33], electrochemically controllable electronic conjugation has wide applications. Furthermore, if solution phase particles are nano-sized then electrode surfaces tend to contain nano-sized pores.

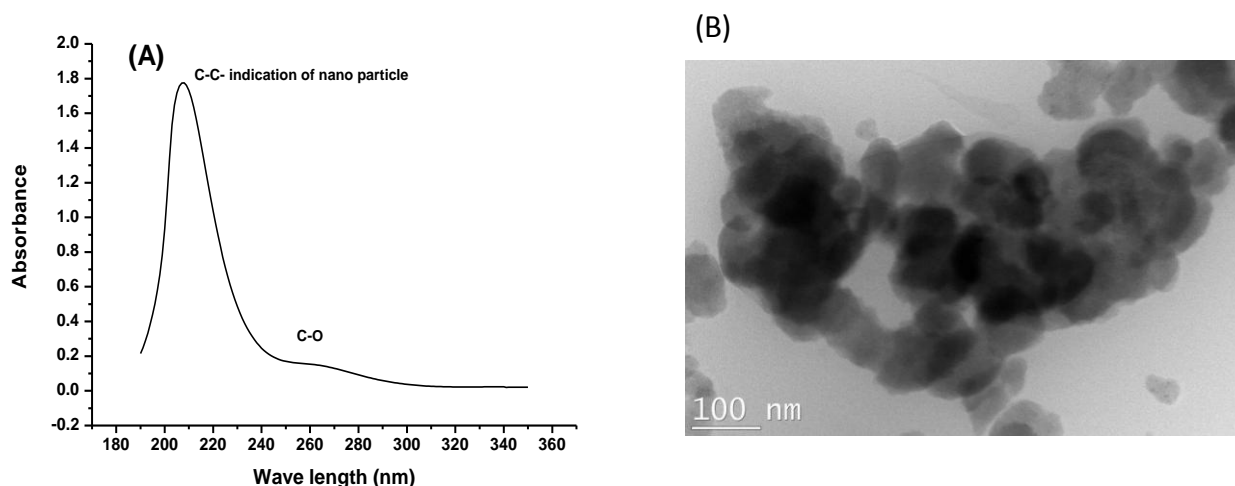


**Figure 2.** (A) UV-Visible spectrum of as prepared graphene oxide dispersed in 2 M NH<sub>3</sub> + 2% 2 M H<sub>2</sub>SO<sub>4</sub> + 1% (v/v) TritonX-100 using an electrochemical bath. Preparation conditions: Applied DC potential = 7.5 V; Duration time = 5 hrs; Electrode = graphite (5 mm diameter) (B) TEM image of graphene oxide nano-particles dispersed in 2 M NH<sub>3</sub> + 2% 2 M H<sub>2</sub>SO<sub>4</sub> + 1% (v/v) TritonX-100 electrochemically. Electrode preparation conditions were the same as those mentioned in Fig.2A.

### 3.2 Surface characterization

The surface elemental compositions of graphite and NP-GO<sub>el</sub> electrodes after preparation were evaluated by XPS analysis (Table 1). The O/C ratio increased from 0.24 to 0.97 for pristine graphite and NP-GO<sub>el</sub>, respectively, is confirming the effectiveness of surface oxidation. The appeared N1s and sp<sup>2</sup> peaks might have been by NH<sub>3</sub> and H<sub>2</sub>SO<sub>4</sub> from electrolyte. In order to identify functional groups and its respective percentages, high resolution XPS spectra and curve-fitted C1s spectra were obtained (Fig. 3). Peak assignments of different functional groups of graphite and NP-GO<sub>el</sub> electrode and their relative contents are detailed in Table 2.

**Table 1.** Atomic ratio of the electrodes

Material	Elements						O/C ratio
	C1s	O1s	Zn2p <sub>3</sub>	Ca2p <sub>3</sub>	N1s	S2p	
Graphite	60.50	14.64	3.00	2.79	-	-	0.24
NP-GO <sub>el</sub>	35.61	34.48	-	-	9.17	3.96	0.97

**Table 2.** Functional groups from deconvoluted XPS spectra of C1s (relative atomic percentage, %)

Sample	C=C(Sp <sup>2</sup> ) (284.5 eV)	C-OH (285.7 eV)	C-O-C(287.8 eV)
Graphite	83.34	13.30	1.27
NP-GO <sub>el</sub>	32.36	45.75	17.22

The content of sp<sup>2</sup>-hybridized carbon was found to decrease sharply from 83.34 % for pristine graphite to 32.36 % for NP-GO<sub>el</sub>, indicating that a large number of oxygen-containing functional groups are generated on NP-GO<sub>el</sub>, such as, hydroxyl (C–OH -285.67 eV) and epoxy (C–O–C-287.79 eV), as show in Fig.3(c & d), the latter of which break carbon  $\pi$  bonds and transforms them into single C–C or sp<sup>3</sup> bonds [34-36]. Almost three times higher of C-OH groups (45.75 %) and sixteen times higher of C-O-C group (17.22 %) were obtained for NP-GO<sub>el</sub> electrode. These findings also suggest that specific or controlled preparation of C-OH and C-O-C oxygen groups is possible using the described electrochemical method, and that other oxygen functional groups like carbonyl (C=O) and acid (COOH) can be avoided. It is noteworthy that graphene oxide modified electrodes means, at this stage, multilayer of graphene oxide nano platelets [23]. If the graphene oxide sheets aligned perpendicularly on the electrode surface such an arrangement may closely resemble to graphene oxide properties. Or monolayer sheet of graphene oxide by perpendicular orientation may be called graphene oxide modified electrode. At present no such like electrode was used but the present electrochemically prepared electrode resembles perpendicularly oriented graphene oxide edge like electrode, as seen in scheme 1. More number of C-O-C and C-OH groups either in or out of plane mimics the graphene oxide [37], and thus, the present method of preparation favors graphene oxide edge like formation. Additionally, AFM analysis was carried out to determine surface pore structures and sizes (Fig.4). 3D

view of normal graphite electrodes showed long voids and rough surface (Fig.4A). On the other hand, graphite oxide electrode contained more number of small voids and pores (Fig.4B).

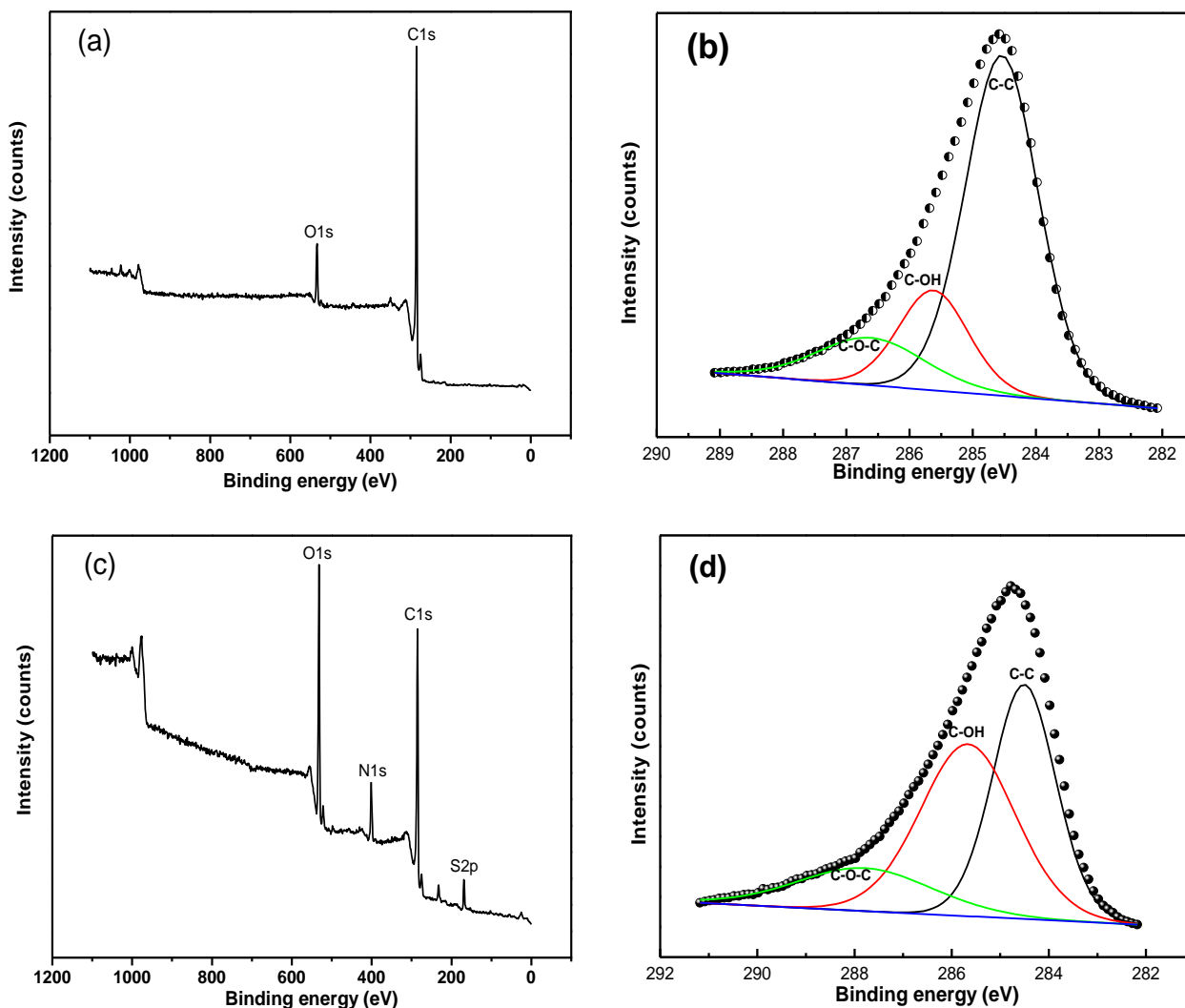
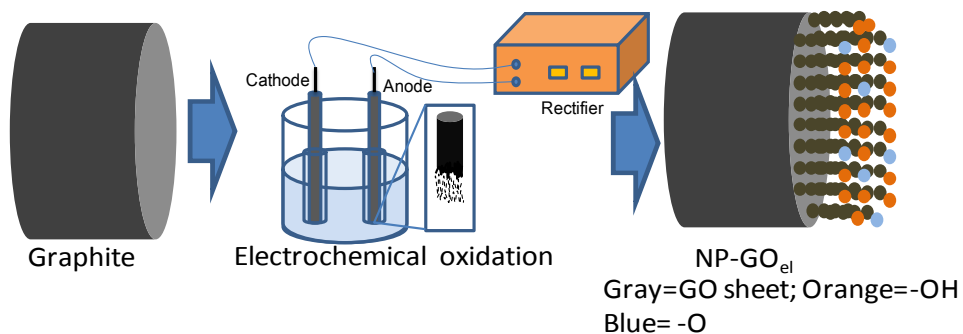


**Figure 3.** XPS survey scan spectra and high-resolution spectra of C1s (a and b) graphite, (c and d) NP-GO<sub>el</sub>. Electrode preparation conditions were the same as those mentioned in Fig.2A.



**Scheme 1.** Pictorial representation of graphene oxide edge like electrode preparation.

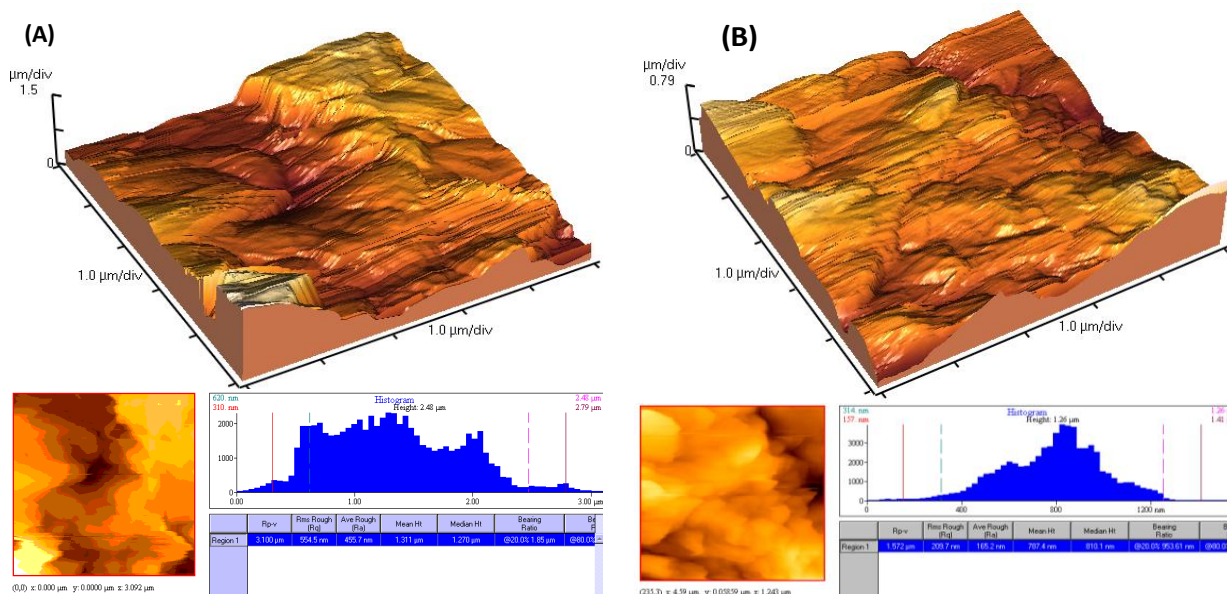


**Figure 4.** AFM images of graphite (A) and NP-GO<sub>el</sub> (B). The bottom panel figures depict the average surface roughness of respective electrodes. Electrode preparation conditions were the same as those mentioned in Fig.2A.

The high resolution AFM image (below each 3D image) of the graphite (Fig.4A) and NP-GO<sub>el</sub> (Fig.4B) electrodes showed that pore sizes varied from 440 to 160 nm, i.e., NP-GO<sub>el</sub> electrode had an average roughness of 160 nm. We believe that voids and holes in the NP-GO<sub>el</sub> electrode were 60 to 80 nm in size at a surface roughness of 160 nm. Our results show that the prepared electrode had nano pores and a graphene oxide edge like in nature.

### 3.3 Electrochemical characterization of NP-GO<sub>el</sub> on Cerium redox couple

The cyclic voltammetry (CV) responses of CeIV/CeIII redox couple at three different graphite electrodes that prepared using the potential cycling, CP electrolysis in 2 M NH<sub>3</sub>, and CP electrolysis in 2 M NH<sub>3</sub>+ 2% 2 M H<sub>2</sub>SO<sub>4</sub> + 1% triton-100 methods were studied at 20 mVs<sup>-1</sup> (Fig.5). First, graphite electrode pretreated using the potential cycling method, cycling between -0.5 V to 1.0 V for 5 cycles, in neutral pH solution and then CV responses were recorded in 0.1 M Ce<sup>3+</sup> in 1 M MSA solution, showed an oxidation potential of 1.53 V and a reduction potential of 1.4 V (Fig.5 curve a). The peak potential difference ( $\Delta E_p$ ) of the graphite pretreated using potential cycling method was 130 mV, and this follows highly quasi-reversible in nature [38]. In the case of the electrode prepared using the CP method in the presence of 2 M NH<sub>3</sub> solution, CV response showed a peak potential difference of 150 mV, also indicating a quasi-reversible electron transfer process. At the same time, the electrode prepared in presence of 2 M NH<sub>3</sub>+ 2% 2 M H<sub>2</sub>SO<sub>4</sub> + 1% triton-100 using CP electrolysis method showed a highly reversible electron transfer process, in other words a rapid electron transfer process with a peak potential difference of almost 60 mV (Fig.5 curve c), which is for one electron transfer process [38]. The above results provide evidence that CeIV/CeIII is highly reversible for the electrode

prepared in 2 M  $\text{NH}_3$  + 2 M 2%  $\text{H}_2\text{SO}_4$  + 1% TritonX-100 solution and that this may be due to the presence of more oxygen functional groups. This is consistent with reports issued by Sun and Skyllas-Kazacos [23, 39], who found that the functional groups C–OH and C–O–H catalyze the redox reaction by generating active reaction sites. Additionally, a higher charging current (base current) was evident in Fig.5 curve c than for the other two preparation conditions, indicating that a larger number of pores was formed (nano pores as in Fig.4).

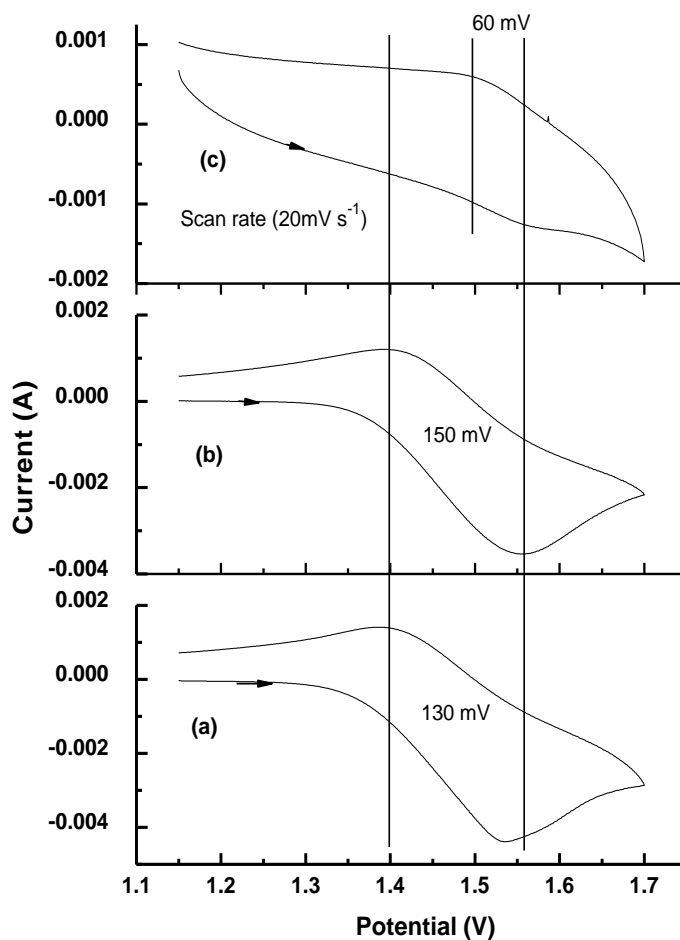


**Figure 5.** Cyclic voltammograms of a graphite electrode prepared by potential cycling method (a), a graphite oxide prepared in 2 M  $\text{NH}_3$  (b), NP-GO<sub>el</sub> prepared in 2 M  $\text{NH}_3$  + 2% 2 M  $\text{H}_2\text{SO}_4$  + 1% (v/v) TritonX-100 (c) obtained at a scan rate of 20  $\text{mVs}^{-1}$  in 0.1 M  $\text{CeSO}_4$  + 1 M MSA.

Moreover, the diffusion tail (current behavior after oxidation (anodic) peak) was almost zero for curve c in Fig.5, indicating that the diffusion layer thickness was low; this is happened only under dynamic electrode conditions or when the electrode was rotated [40]. Because of over grapheme oxides with nano pores on the electrode surface, linear diffusion becomes non-linear diffusion or nearly steady state condition (mass transfer phenomena) at interface [41]. Based on the above results, the prepared electrode appears suitable as a NP-GO<sub>el</sub> electrode. The reaction mechanism is presumed to be as follows.



### 3.4 Electrochemical characterization of Nafion coated NP-GO<sub>el</sub> electrodes

Fig.6(A) shows the CV response of a Nafion coated-NP-GO<sub>el</sub> electrode under different scan rates in 0.1 M Ce + 2 M MSA. The figure shows that peak potential separation increases with scan rate. This may be due to deviation from diffusion controlled electron transfer phenomena at higher scan rates and morphological change due to oxygen functional group changes. SEM images (Fig.6(B)) of both pure NP-GO<sub>el</sub> and Nafion coated NP-GO<sub>el</sub> (first 5 cycles) showed no prominent differences in electrode morphology that might explain the peak potential increase only from deviation from diffusion controlled electron transfer at higher scan rates.

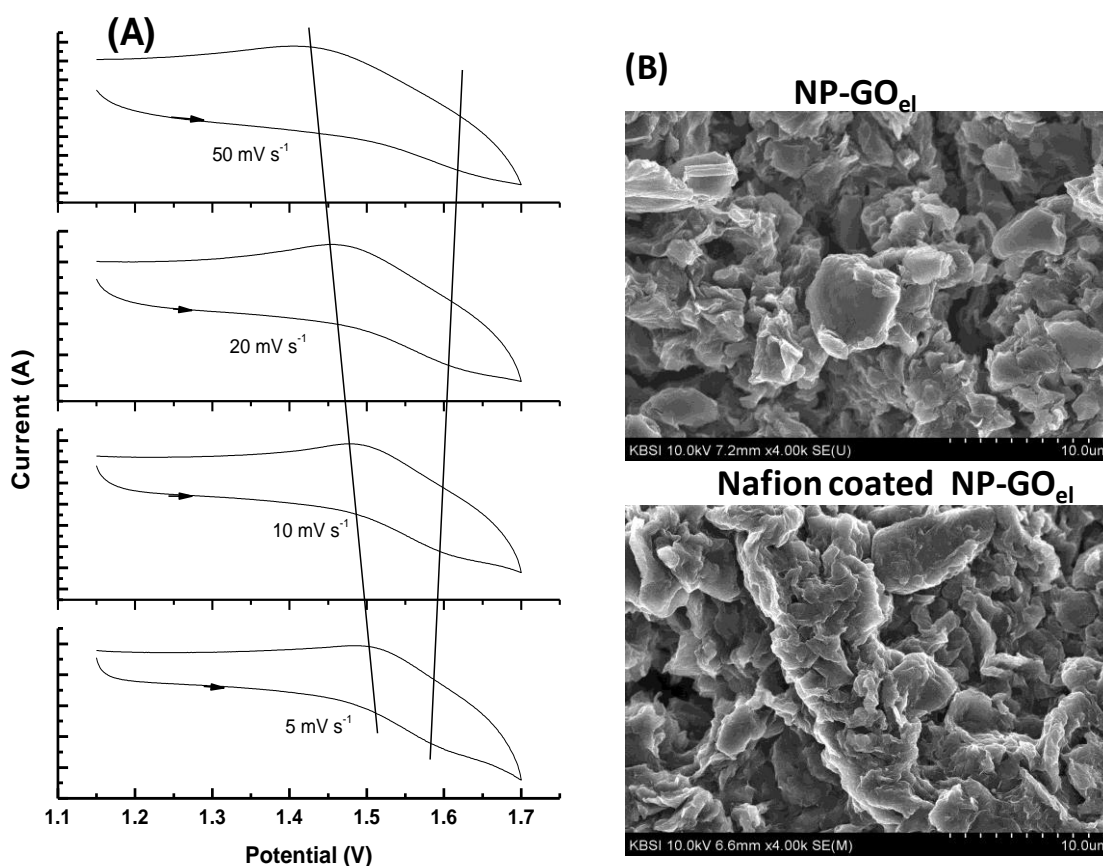


**Figure 6.** (A) Cyclic voltammograms of Nafion coated NP-GO<sub>el</sub> under different scan rates in 0.1 M CeSO<sub>4</sub> + 2 M MSA. (B) SEM images of NP-GO<sub>el</sub> (a) and Nafion coated NP-GO<sub>el</sub> (b).

As mentioned in the introduction, the stability of the anode should be another more important for cerium oxidation because the high oxidation potential (1.56 V) leads to the dissolution of carbon particles. The Nafion coated NP-GO<sub>el</sub> was tested at a scan rate of 50 mVs<sup>-1</sup> in 0.1 M Ce + 2 M MSA,

results are depicted in Fig.7. The oxidation/reduction peak current of Ce(III)/Ce(IV) slightly decreases with cycle number (over the first 5 cycles). This slow decrease in oxidation/reduction peak current continued up to 300 cycles and then stopped, as shown in the inset in Fig.7. This explains the greater stability of Nafion coated-NP-GO<sub>el</sub> on cerium oxidation/reduction. The prepared Nafion coated NP-GO<sub>el</sub> electrode appears to be a good alternative for real Ce-V RFB applications.

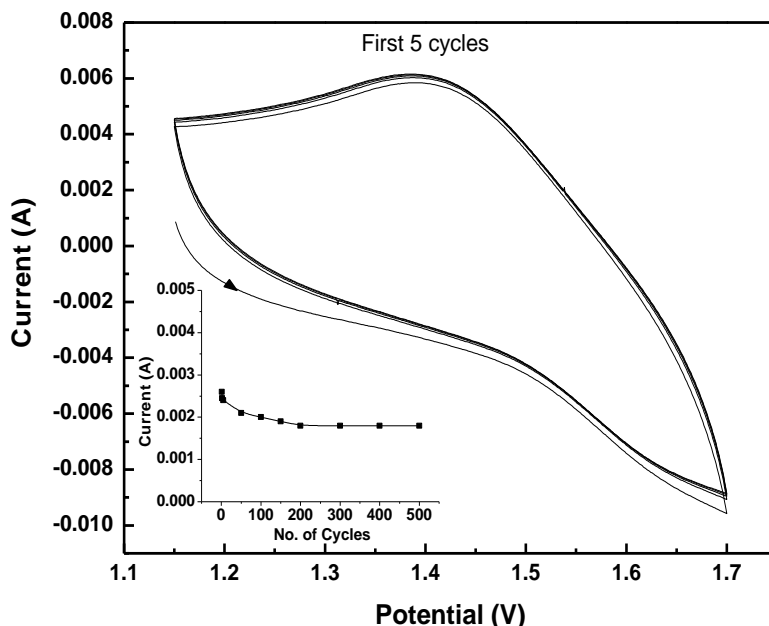


**Figure 7.** Cyclic voltammograms of Nafion coated NP-GO<sub>el</sub> under continuous cycling at a scan rate of 50 mVs<sup>-1</sup> in 0.1 M CeSO<sub>4</sub> + 2 M MSA. Inset: Anodic peak current (baseline corrected) variation with number of cycles (Potential at 1.62 V).

#### 4. CONCLUSIONS

An NP-GO<sub>el</sub> electrode was successfully prepared using a modified electrochemical method for Ce-V redox RFB applications. UV-Vis and TEM analysis indirectly confirmed the presence of nano pores prepared using CP electrolysis method in presence of 2 M NH<sub>3</sub>+ 2% 2 M H<sub>2</sub>SO<sub>4</sub> + 1% triton-100 solution medium. In addition, along with the nano pores, NP-GO<sub>el</sub> contains C-OH and C-O-C groups on surface were confirmed by AFM and XPS analysis. NP-GO<sub>el</sub> electrodes demonstrated better electrocatalytic activity towards Ce(IV)/Ce(III) redox couples than normally activated graphite electrodes. The catalytic effect of NP-GO<sub>el</sub> with respect to the oxidation of Ce(III) was attributed to the formation of surface active functional groups (C-OH and C-O-C) and nano pores. In addition, a Nafion coating on NP-GO<sub>el</sub> electrodes was found to increase durability. These encouraging results suggest that NP-GO<sub>el</sub> electrodes are promising candidates for Ce-V RFBs.

## ACKNOWLEDGEMENTS

This work was supported by the Ministry of Trade, Industry and Energy (MOTIE) through the project of GTFAM Regional Innovation Center (RIC) and National Research Foundation of Korea (NRF) funded by the Korea government (MEST) (Grant No. 2010-0027330).

## References

1. M. Gattrell, J. Park, B. MacDougall, J. Apte, S. McCarthy and C. W. Wu, *J. Electrochem. Soc.* 151 (2004) 123–130.
2. C. Fabjan, J. Garche, B. Harrer, L. Jorissen, C. Kolbeck, F. Philippi, G. Tomazic and F. Wagner, *Electrochim Acta* 47 (2001) 825–831.
3. F. Rahman and M. Skyllas-Kazacos, *J. Power Sources*. 189 (2009) 1212-1219.
4. M. Gattrell, J. Qian, C. Stewart, P. Graham and B. MacDougall, *Electrochim. Acta* 51 (2005) 395-407.
5. S. H. Pawar, R. D. Madhale, P. S. Patil and C. D. Lokhande, *Bull. Mater. Sci.* 10 (1988) 367-372.
6. M. Rychcik and M. Skyllas-Kazacos, *J. Power Sources* 22 (1988) 59-67.
7. L. W. Hruska and R. F. Savinell, *J. Electrochem. Soc.* 128 (1981) 18-25.
8. B. Fang, S. Iwasa, Y. Wei, T. Arai and M. Kumagai, *Electrochim. Acta* 47 (2002) 3971-3976.
9. R. L. Clarke, B. J. Dougherty, S. Harrison, P. J. Millington and S. Mohanta, *US pat.*, 0202925A1 (2004).
10. X. Xia, H.-T. Liu and Y. Liu, *J. Electrochem. Soc.* 149 (2002) A426-A430.
11. P. K. Leung, d. L. C. Ponce, C. T. J. Low and F. C. Walsh, *Electrochim. Acta* 56 (2011) 2145-2153.
12. Y. Wei, B. Fang, T. Arai and M. Kumagai, *J. Appl. Electrochem.* 35 (2005) 561-566.
13. P. Trinidad, C. P. de Leon and F. C. Walsh, *J. Environ. Manage.* 88 (2008) 1417-1425.
14. Y. Liu, X. Xia and H. Liu, *J. Power Sources* 130 (2004) 299-305.
15. W. H. Wang and X. D. Wang, *Electrochim. Acta* 52 (2007) 6755-6762.
16. H. Kaneko, K. Nozaki, Y. Wada, T. Aoki, A. Negishi and M. Kamimoto, *Electrochim. Acta* 36 (1991) 1191-1196.
17. H. Q. Zhu, Y. M. Zhang, L. Yue, W. S. Li, G. L. Li, D. Shu and H. Y. Chen, *J. Power Sources* 184 (2008) 637-640.
18. G. J. W. Radford, J. Cox, R. G. A. Wills and F. C. Walsh, *J. Power Sources* 185 (2008) 1499-1504.
19. Y. Liu, X. Xia and H. Liu, *J. Power Sources* 130 (2004) 299-305.
20. P. K. Leung, C. Ponce-de-Leon, C. T. J. Low, A. A. Shah and F. C. Walsh, *J. Power Sources* 196 (2011) 5174-5185.
21. A. Zhamu and B. Z. Jang, p. 23pp., Chemical Indexing Equivalent to 155:129751 (WO) (2011).
22. T. S. Szabo, A. Szeri and I. Dekany, *Carbon* 43 (2005) 87-94.
23. B. Sun and M. Skyllas-Kazacos, *Electrochim. Acta* 37 (1992) 1253–1260.
24. D. A. C. Brownson and C. E. Banks, *Analyst* 135 (2010) 2768-2778.
25. W. Li, J. Liu and C. Yan, *Electrochim. Acta* 56 (2011) 5290-5294.
26. Y. Zhu, S. Murali, W. Cai, X. Li, J. W. Suk, J. R. Potts and R. S. Ruoff, *Adv. Mater.* 22 (2010) 3906-3924.
27. P. Han, H. Wang, Z. Liu, X. Chen, W. Ma, J. Yao, Y. Zhu and G. Cui, *Carbon* 49 (2011) 693-700.
28. M. Pumera, A. Ambrosi, A. Bonanni, E. L. K. Chng and H. L. Poh, *Trends Anal. Chem.* 29 (2010) 954-965.
29. H.-W. Hu, G.-H. Chen, M. Fang and W.-F. Zhao, *Synth. Met.* 159 (2009) 1505-1507.
30. F. Zeng, Z. Sun, X. Sang, D. Diamond, K. T. Lau, X. Liu and D. S. Su, *ChemSusChem* 4 (2011) 1587-1591.
31. D. A. Skoog, F. J. Holler and T. A. Nieman, *Principles of Instrumental Analysis*. Hartcourt Brace & Company, Philadelphia, 5<sup>th</sup> edn, (1998).

32. D. Li, M. B. Muller, S. Gilje, R. B. Kaner and G. G. Wallace, *Nat Nano* 3 (2008) 101-105.
33. M. Zhou, Y. Wang, Y. Zhai, J. Zhai, W. Ren, F. Wang and S. Dong, *Chem. – A Eur. J.* 15 (2009) 6116-6120.
34. T. Szabo, E. Tomba'cz, E. Ille's and I. De'ka'ny, *Carbon* 44 (2006) 537–545.
35. H. M. Ju, S. H. Huh, S. H. Choi and H. L. Lee, *Mater. Lett.* 4 (2010) 357–360.
36. D. Yang, A. Velamakanni, G. I. Bozoklu, S. Park, M. Stoller, R. D. Piner, S. Stankovich, I. Jung, D. A. Field, C. A. Ventrice Jr and R. S. Ruoff, *Carbon* 47 (2009) 145-152.
37. J. Zhao, S. Pei, W. Ren, L. Gao and H. M. Cheng, *ACS Nano* 4 (2010) 5245-5252.
38. A. J. Bard and L. R. Faulkner, *Electrochemical Methods: Fundamental and Applications*, John Wiley & Sons, New York, 1<sup>st</sup> edn, (1980).
39. B. Sun and M. Skyllas-Kazacos, *Electrochim.Acta* 37 (1992) 2459–2465.
40. P. R. Unwin and R. G. Compton, *J. Electroanal. Chem. Interf. Electrochem.* 245 (1988) 287-298.
41. R. M. Wightman and D. O. Wipf, *Voltammetry at ultramicroelectrodes*. ed. A. J. Bard, Electroanalytical chemistry, Marcel Dekker, New York (1988) vol.15, p. 267-353.